

# Study of Heat Transfer and Friction Factor Correlation on Broken ACR Roughness Elements on the Absorber Plate for Solar Energy Based Heater: A Review

Ishwar Chandra, Sanjeev Kumar Yadav, Sumit Kumar

**Abstract**— Solar air heater performance can be enhanced by adding roughness to the inner periphery. The present study is based on the various shape parameters for broken arc shape roughness element of heat transfer and friction factor characteristics of the rectangular duct roughened with repeated square cross-section broken ribs with a gap. Duct has width to height ratio ( $W/H$ ) of 5, relative roughness pitch ( $P/e$ ) of 8, relative roughness height ( $e/D$ ) of 0.045 and the arc angle ( $\alpha$ ) of  $60^\circ$ . In the range of 0.5-1 gap width ( $g/e$ ) and 0.16-0.66 gap position ( $d/w$ ) are varied. Under the similar flow condition heat transfer and friction factor of smooth duct is compared with roughness duct. The duct has Reynolds number ( $Re$ ) range of 3000-22300. The maximum enhancement in Nusselt number and friction factor is obtained by 6.74 and 6.73 times.

**Index Terms**— Heat Transfer, Friction factor, Broken arc, Solar energy, Reynolds number, Nusselt number.

## I. INTRODUCTION

The convective heat transfer coefficient between air and the absorber plate is low. Convective heat transfer is low due to presence of sub-layer and the thermal performance of solar air heater is poor. Which can be broken by artificial roughness on heat transfer surface [1]. Conversion of solar energy into thermal energy is the easiest way for heating application with the use of solar air heater. By artificial roughness friction losses lead to excess power requirement for the fluid to flow through the duct. The turbulence must be created only in a region very close to the heat transfer surface to break the viscous sub-layer for augmenting the heat transfer. The effect of rib shape angle of attack pitch to rib height ratio ( $P/e$ ) on friction factor and heat transfer characteristics for rectangular shape with two side roughness wall..

Lots of study on heat transfer has been performed on several years [3-5]. An idea about some roughness in heat transfer can be lead to turbulence flow like situation in the region and issue of low heat transfer coefficient can be addressed reasonable. Solar radiation incident is absorbed by solar collector and it converted into heat for heating the fluid (air or water). Their low efficiency is negative effect which is

reasonable due to low convective heat transfer coefficient between air flow and absorber plate by which increased absorber plate temperature. Yadav et al.[7] studied the influence of Reynolds number on the surface having array externally shape on heat transfer coefficient distribution. The enhancement in Nusselt number and friction factor is absorbed to be 2.5 times of that of smooth surface. Sethi et al.[8] has carry one experimental investigation on dimple shape roughness used in solar air heater. The relation developed between Nusselt number and friction factor Kumar et al.[9] carried experimental research of friction and heat transfer in the flowing air in rectangular duct having v-shape ribs with gap roughness on the absorber plate. By experimentally Nusselt number and friction factor increased by maximum 6.74 and 6.73 times. Here correlation also developed between Nusselt number and friction factor. Karwa and Chitoshiya[10] has experimental carry study of performance of thermo hydraulic of solar air heater with  $60^\circ$  v-down discrete rib roughness of the absorber plate on the side of air flow along with smooth duct solar air heater. The enhancement of Nusselt number was maximum 2.3 times and characteristics of friction were 2.83 times compared with smooth duct. Hans et al[12] carried out the effect of multiple v-ribs over the absorber plate and generate the relation between Nusselt number and friction factor.

The investigation carried out the heat transfer rate and friction factor is purpose to heating of air in rectangular duct having multiple broken arc shape as roughness geometry. By experimental the relation developed between Nusselt number and friction factor. The investigation is given in figure1. By patching aluminium wires in multiple arc shape fashion the roughness geometry has been created under the absorber plate. By which heat transfer characteristics of rough duct have been investigated

The investigations carried out the heat transfer rate and friction factor is purpose to heating of air in rectangular duct having multiple broken arc shaped as a roughness geometry. By experimental the relation developed between Nusselt number and friction factor. The recently investigation is given in figure1. By patching aluminium wires in multiple arc-shape fashion the roughness geometry has been created under the absorber plate. By which heat transfer characteristics of rough duct have been investigated, 25 roughened plates were fabricated and tested. The obtained values are expressed in terms of roughness pitch ( $p/e$ ), relative roughness height ( $e/D$ ), arc angle ( $\alpha$ ) and roughness width ( $W/w$ ). All the obtained values are shown in table1.

**Ishwar Chandra**, Heat Power & Thermal, Department of Mechanical Engineering, Technocrats Institute of Technology, Bhopal, +91-8445295577

**Sanjeev Kumar Yadav**, Heat Power & Thermal, Department of Mechanical Engineering, Technocrats Institute of Technology, Bhopal, +91-9425360919

**Sumit Kumar**, Heat Power & Thermal, Department of Mechanical Engineering, Technocrats Institute of Technology, Bhopal, +91-9368125318

Nomenclature	
$A_p$	surface area of absorber plate ( $m^2$ )
$A_o$	area of orifice meter ( $m^2$ )
$C_p$	specific heat of air ( $J/Kg-K$ )
$C_d$	coefficient of discharge
$D$	hydraulic diameter (m)
$e$	rib height (m)
$b/e$	relative broken width
$e/D$	relative roughness height
$f$	friction factor for roughened duct
$f_s$	friction factor for smooth duct
$h$	height of duct
$K$	thermal conductivity ( $W/m-k$ )
$L$	length of test section in duct (m)
$Nu$	Nusselt number
$Nu_s$	Nusselt number for smooth duct
$\Delta P_o$	pressure drop across the orifice plate (pa)
$\Delta P_D$	pressure drop across the test section (Pa)
$P$	pitch (m)
$p/e$	relative roughness pitch
$Pr$	Prandtl number
$Q_u$	useful heat gain
$Re$	Reynolds number
$T_o$	air outlet temperature (K)
$T_i$	air inlet temperature (K)
$T_{pm}$	average temperature of absorber plate (K)
$T_{fm}$	average temperature of air (K)
$V$	mean flow velocity in duct (m/s)
$W$	width of duct (m)
$W/w$	relative roughness width
$W/H$	aspect ratio of duct
Greek symbols:	
$\alpha$	arc angle ( $^\circ$ )
$\rho$	density ( $kg/m^3$ )
$\beta$	ratio of orifice diameter to pipe diameter

## II. EXPERIMENTAL DETAILS

### 2.1. Materials and Procedures

A rectangular channel have forced convection flow is used in this type of experimental set up. The entrance, test and exit section are 800 mm, 1000 mm and 500 mm respectively and total length of rectangular channel is 2300 mm[1-2]. Wooden rectangular duct, electric heater, GI pipe, control valves, blower, orifice plate, U-tube manometer, micro-manometer, variable transformer, ammeter, voltmeter, thermo couples and milli-voltmeter are the components of this experimental setup shown in fig.2. The dimensions of inner section are 2300 mm x 330 mm x 30 mm. Having cross-section of 1000 mm x 330 mm an electric heater is provided. Heating wire on a 5 mm thick asbestos sheet is obtained by arrangement in series and parallel loops. For uniformly relation between absorber plate and electric heater thickness of 1 mm mica sheet electric heater wire is provided. Variation of heat flux in between 0 to 1000  $W/m^2$  is used for variable transformer. A glass wood is kept inside the 6 mm thick wooden panel for decrease top loss from heater as insulating materials, 12 thermo couple for plate temperature measurement and 8 thermo couple for inside temperature measurement of duct. For the measurement of the temperature total 20 thermo couples are provided. U-tube manometer is connected to orifice meter for measurement of

mass flow rate of air in the rectangular duct. A valve is used to control the flow, is called control valves. A digital voltmeter is provided for output measurement of the thermo couples. Micro manometer is also used to measure pressure drop in test section and its least count is 0.01 mm of water. Micro manometer, U-tube manometer, milling-voltmeter, voltmeter and ammeter are used for finding the function the function is in proper way or not and check to all joint, there is no any leakage in the system. After verified, blower switched on. By control valve of Reynolds number, mass flow rate is arranged. Reading was taken in quasi steady process. Quasi- steady means slow changes in system that means temperature will be steady for 10-15 minute. In order to Reynolds number different values of mass flow rate of air was obtained. The following parameters are found by experiment: pressure drop across orifice plate, pressure drop across test section, inlet air temperature, outlet air temperature and the temperature of the plate.

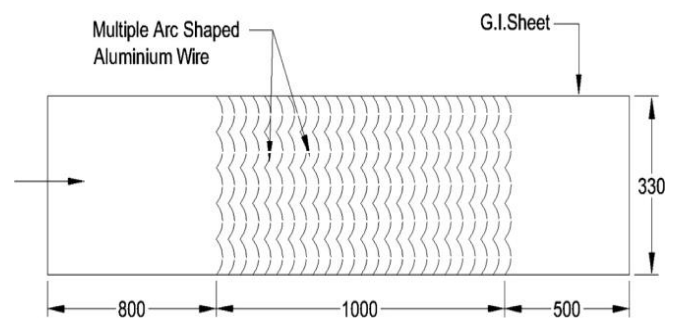


**Fig.1.** roughened multiple broken absorber plate.

The equation are used for finding the values of heat transfer coefficient 'h', useful heat gain ' $Q_u$ ', Nusselt number ' $Nu$ ', Reynolds number ' $Re$ ', friction factor ' $f$ ' and thermo hydraulic performance parameter ' $\eta$ ':

Mass flow rate  $m$  has been found by pressure drop across the orifice plate

$$M = C_d A_o \sqrt{\frac{2\rho\Delta P_o}{1-\beta^4}} \quad (1)$$

where coefficient of discharge  $C_d$  is 0.605 by calibrate.

And  $\Delta P_o = 9.81\rho_m\Delta h_o\sin\theta$ . Where  $\theta = 90^\circ$  for this (2)

Hence,

$$\Delta P_o = 9.81\rho_m\Delta h_o \quad (3)$$

Friction factor is calculated by

$$f = \frac{2\rho_w g \Delta h_d}{4\rho L V^2} \quad (4)$$

Where  $\Delta P_D = \rho_w g \Delta h_d$ ,  $\Delta h_d$  is head loss across the test section length of 1 m.

And

$$D = \frac{4WH}{2(W+H)}$$

Nusselt number ( $Nu$ ) is calculated by

$$Nu = hD/k \quad (5)$$

$$H = Q_u/A_p(T_{pm}-T_{fm}) \quad (6)$$

where, ' $Q_u$ ' is rate of heat given by air, ' $A_p$ ' is the area of the absorber plate, ' $T_{fm}$ ' is average value of the air temperature and ' $T_m$ ' is absorber plate temperature.

$$Q_u = mC_p(T_o - T_i) \quad (7)$$

From above all these calculation, air properties corresponding to bulk mean air temperature is used. By Kline and McClintock[14] method value will be calculated. By the

analysis of error estimation through various instruments, the values of non dimensional number are calculated: Reynolds number  $\pm 2.20\%$ , Nusselt number  $\pm 4.90\%$ , friction factor  $\pm 3.82\%$  and Stanton number is  $\pm 3.67\%$ .

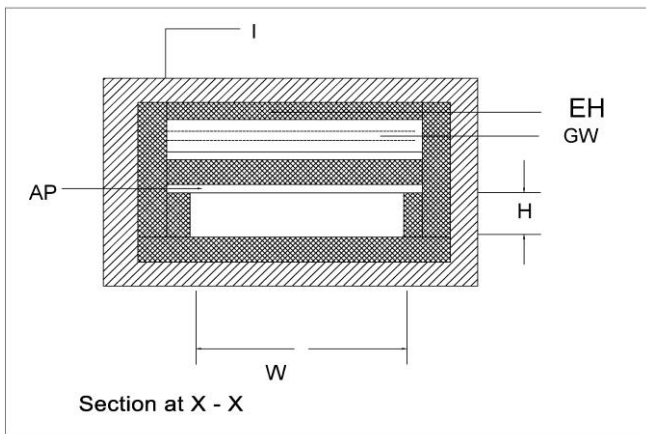
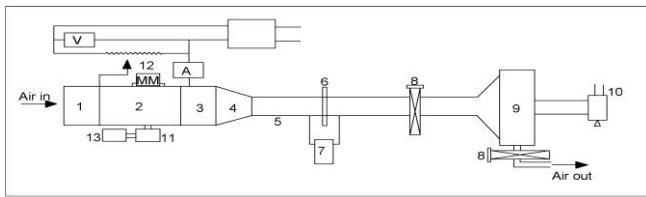


Fig2. Schematic diagram of experimental set up.

- |                         |                      |               |
|-------------------------|----------------------|---------------|
| A-Ammeter               | EH-Electric heater   | H-Duct height |
| V-Voltmeter             | GW-Glass wool        | W-Duct width  |
| MM-Micro-Manometer      | I-Insulation         |               |
| AP-Absorber Plate       |                      |               |
| 1. Entry section        | 8. Control valve     |               |
| 2. Test section         | 9. Blower            |               |
| 3. Exit Section         | 10. Electric motor   |               |
| 4. Transition section   | 11. Selector switch  |               |
| 5. G.I.Pipe transformer | 12. Variable         |               |
| 6. Orifice meter        | 13. Milli-voltmeter. |               |
| 7. U-tube manometer     |                      |               |

## 2.2. Validity Test

Compare the value of Nusselt number and friction factor by experimental data for smooth duct to the obtained value from Dittus-Boelter[15] and modified Blasius equation[16].

Nusselt number for smooth rectangular duct is obtained by Dittus-Bolter equation as

$$Nu_s = 0.023 Re^{0.8} Pr^{0.4}$$

(8) Friction factor for smooth duct is obtained by modified Blasius equation

$$f_s = 0.085 Re^{-0.25}$$

(9)

Comparison of the experimental and estimated value for Nusselt number as a function of Reynolds number as shown in fig.3(a) and friction factor is function of the Reynolds number in fig.3(b).The average variation in Nusselt number from experimental value is obtained from equation(8)

and average variation in friction factor from experimental value is obtained from(9). The accuracy of data is obtained by experimental set up of these two sets of values.

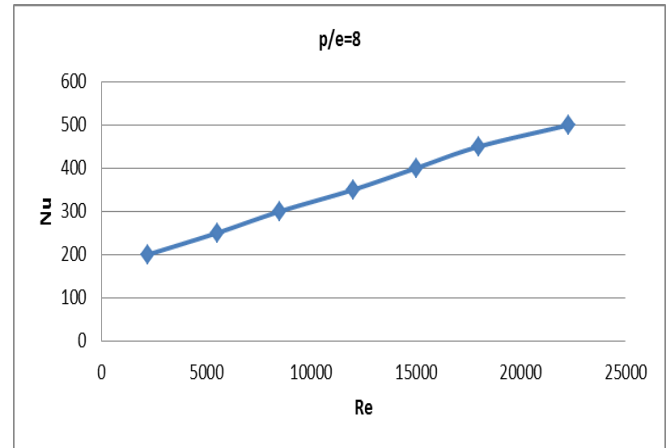


Fig.3. (a) Experimental and estimated values of Nusselt number of smooth duct.

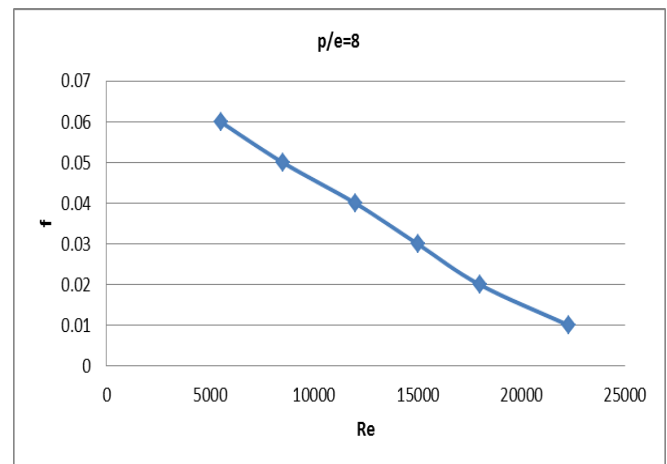


Fig.3.(b) Experimental and estimated values of friction factor of smooth duct.

## III. RESULT AND DISCUSSIONS

The heat transfer and friction factor of rectangular duct having a heated wall and roughness with multiple broken arc shape rib is found by experiments for various roughness working parameters. Effect of various parameters on Nusselt number and friction factor comes in this section.

### 3.1. Reynolds number

Figure.3 (a) and 3(b) shows the effect of Reynolds number (Re) and friction factor (f) on the Nusselt number (Nu). For multiple broken arc shape roughness geometry have pitch roughness (P/e) = 8 and other parameters are relative roughness height (e/D) = 0.045, arc angle ( $\alpha$ ) = 60° and relative broken width (W/w) = 1 kept constant. These result also compared with smooth duct result. Figure 3(a) shows the value of Nusselt number is increases in all Reynolds number. Due to this experimental value with the increase in Reynolds number, turbulence increases which leads to increase the heat transfer whereas friction factor decrease with increase in Reynolds number, which is shown in figure 3(b). Suppression of laminar sub layer for fully developed flow in the duct, pressure drop along the duct increases which leads to high pumping power.

The comparison experimental values and predicted values of Nusselt number and friction factor is shown in fig.4. This graph shows the values for smooth plate in a single graph with lines.

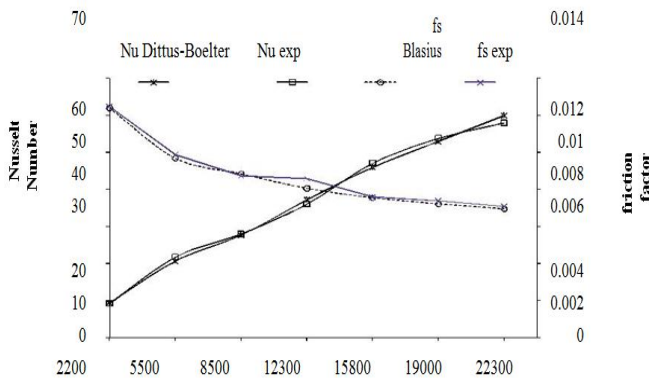


Fig.4. Comparison of experimental and predicted values of Nusselt number and friction factor for smooth plate.

Fig5. Shows the value of Nusselt number as a function of broken width ( $g/e$ ) for different relative broken position ( $b/w$ ) for  $60^\circ$  inclined ribs duct roughness at selected Reynolds number. By observing at any relative broken width the Nusselt number is the height for relative broken position of 0.25 for all Reynolds number.

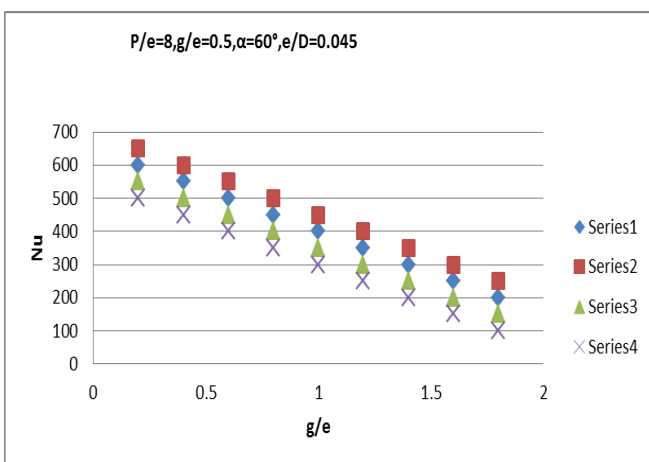


Fig.5. Effect of relative broken width and relative broken position on Nusselt number at fixed Reynolds number.

In fig(6) and fig(7) shows the Nusselt number and friction factor with respect to relative roughness height( $e/D$ ) for different range  $Re$  from 2200 to 22300. The other parameters are  $W/w = 5, \alpha = 60^\circ, p/e = 8$ . From the conclude that the value of  $Nu$  and  $f$  increases with increase in  $e/D$  for all the values of Reynolds number ( $Re$ ) due to increase in  $e/D$ . The fact is relative roughness height value increases, roughness geometry produces more into the flow which causes more turbulence result is increase in Nusselt number ( $Nu$ ) and friction factor( $f$ ). The diagram also shows that the rate of increase of Nusselt number is lower than that of friction factor ( $f$ ). The fact is higher value of  $e/D$  the reattachment free shear might not occur and the rate of heat transfer ( $Q$ ) is not proportional to frictional factor.

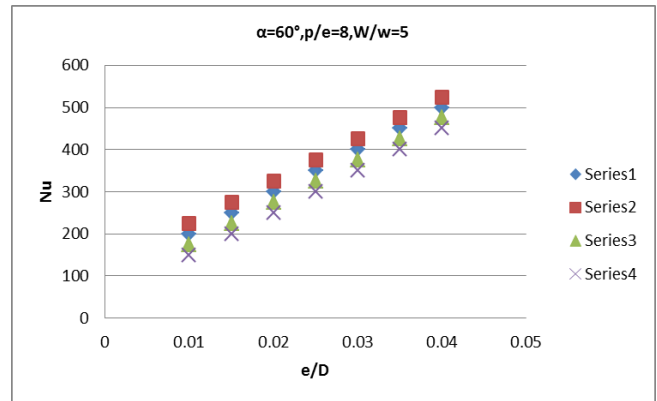


Fig.6. Effect of Nusselt number and  $e/D$  at various Reynolds number.

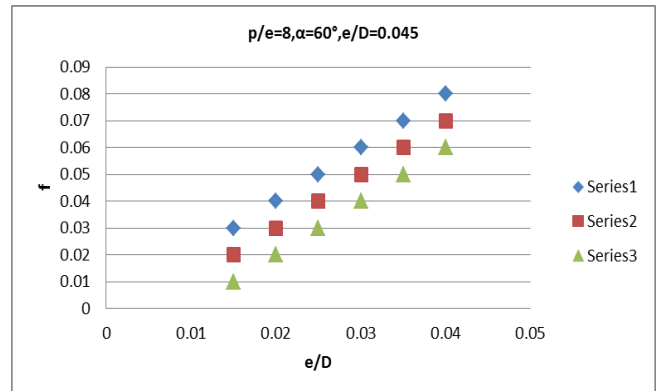


Fig.7. Effect of friction factor and  $e/D$  at various Reynolds number.

compared the Nusselt number of with or without broken multiple arc of the inclined rib with that of the smooth duct. The value of Nusselt number ratio( $Nu/Nu_s$ ) for different value of relative broken position shown in fig(8) and relative broken width is shown in fig(9). The ratio of Nusselt number increases with increase in relative broken width up to 1.0 beyond which it decreases with increase in relative broken width. Nusselt number ratio is high for relative broken width 1.0 and low for 2.0, because increase the relative broken width beyond 1.0, the flow velocity through the broken will reduces, which not be strong to accelerate the flow through the broken and then the heat transfer due to this flow not be increase continuously in compared with that of the continuous ribs. When reduces the broken width lower than 1.0 (i.e  $b/e = 0.5$ ). It may leave very small space for flow of the fluid through it, which is low turbulence and hence reduce the enhancement of heat transfer.

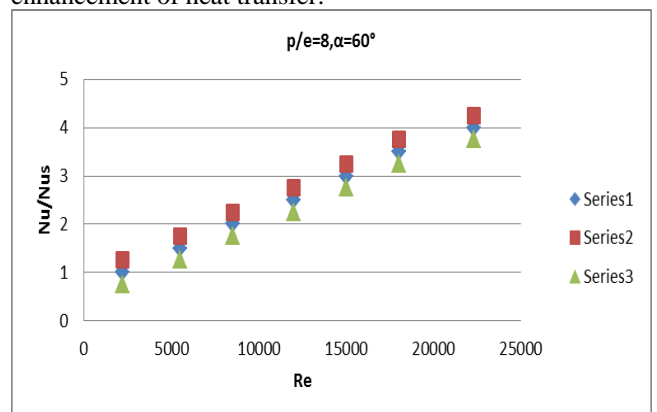


Fig.8. Effect of relative gap position on Nusselt number ratio.

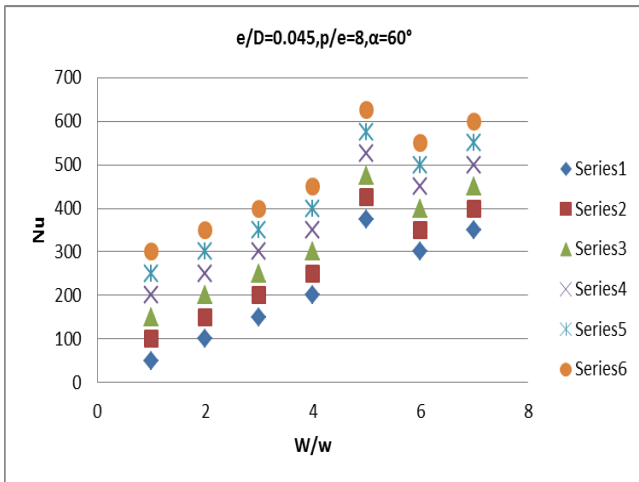


Fig.9. Effect of relative gap position on Nusselt number.

The effect of relative broken position ( $b/w$ ) on the Nusselt number ratio for a fixed relative broken width ( $b/e$ ) of 1.0 is shown in fig. For any Reynolds number it can be obtained the Nusselt ratio is higher for a broken continuous rib as compared with without broken rib and the Nusslet number ratio increase with increase in relative broken position from 0.25 to 1.0, attains a maximum at broken position of 1.0 and after this it decrease with increase in relative broken position. The Nusselt number ratio lies in between 1.7-2.58, under similar condition. The variation of Nusselt number with relative gap position it presented in fig. By which brings out the effect of gap position. Phenomena of flow is in rectangular duct a continuous inclined rib gives rise to secondary flow along with rib length, which gives the working fluid to travel from leading edge to trailing edge of the rib. Flow along the ribs is heated continuously and the boundary layer grows thicker. The flow turns downwards from the side wall and it completes the recirculation loop.

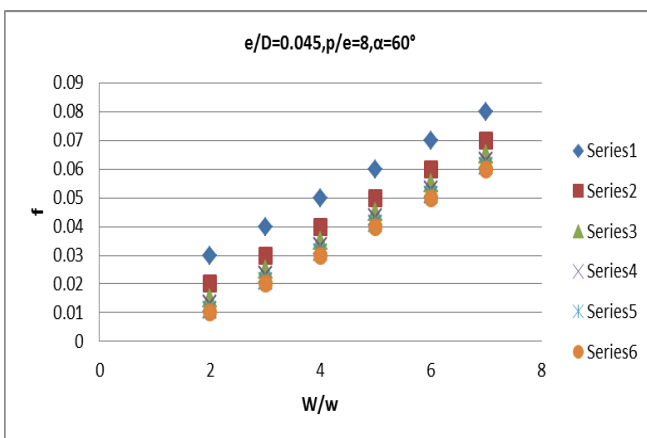


Fig.10. Effect of friction factor and  $W/w$  at Various Reynolds number.

Fig(10) shows the relative roughness width( $W/w$ ) on friction factor( $f$ ). The friction factor have been plotted is function of  $W/w$  for various Reynolds number ( $Re$ ). The other parameters are  $e/D=0.045$ ,  $\alpha=60^\circ$  and  $p/e=8$ . It has been observed that friction factor ( $f$ ) increases with increase in relative roughness width ( $W/w$ ) and its maximum value of  $W/w$  value of 7. The angling of wire help in formation of secondary flow which promotes turbulence mixing and then  $Nu$  increases. A single arc along width of duct which having  $W/w$  value of 1 and considerable improve in heat transfer of

duct as a compared with smooth one. By increase the number of arc would increases the number of secondary flow leads to increase in heat transfer and friction factor. The value of  $W/w$  beyond 5 may result in separation of flow from ribs surface and generate secondary layer which reduces heat transfer. The friction factor increasing on basis of formation of vortices due to separation of flow.

Fig(11). Further investigated mechanism of enhancement of heat transfer as a result of creating gap, ingestion also had been carried out on transverse rib roughness surface with or without a gap of ribs. For the study take two relative gap position ( $g/e$ )=0.25 and 0.5 with relative gap width 1.0, have compared in heat transfer for the case of continuous rib. Fig(10) shows the variety of  $Nu$  with  $Re$  for transverse ribs with or without gap. In this fig seen that there is no significant change in  $Nu$  for continuous rib with a gap. It shows that the creation of gap in transverse ribs does not result significant increase in heat transfer in case of transverse ribs. Increase in heat transfer in case of inclined ribs can be fully attributed to present of secondary flow. However Lalu et al[ ] reported that a  $90^\circ$  discrete rib arranged in staggered manner on the rough plane with a gap between the ribs element by which heat transfer is 10-15% compared to  $90^\circ$  continuous rib arrangement. The reason is enhancement of heat transfer due to the separation of fluid through the end of the discrete rib.

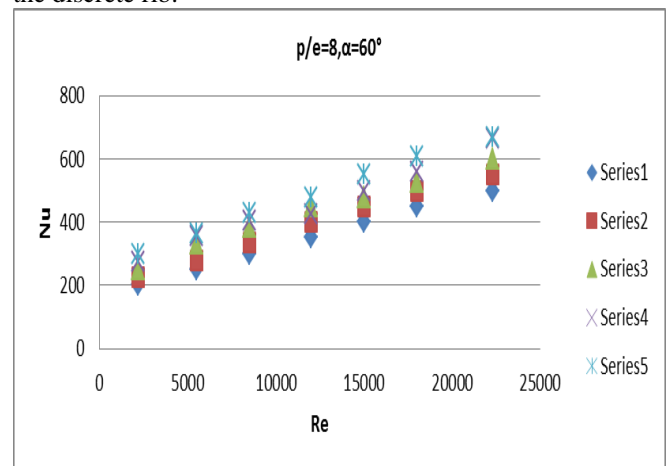


Fig.11. Effect of Nusselt number at Various Reynolds number.

### 3.2. Friction factor:

Axial flow profile is distributed by the secondary flow measurable effect by which increase the friction coefficient in non-circular duct [1]. The lower value of friction factor has been repeated for discrete ribs compared to the continuous ribs [18], due to abbreviate secondary flow cells. Effect of the relative broken width on the friction factor of rough ducts with Reynolds number at broken position of 0.25 is represent in fig [12] in the term of friction factor ratio ( $f/f_s$ ). By which cleared that the friction factor ratio increases with increase in Reynolds number due to increase in the turbulence flow, while this ratio increase with increase in relative broken width upto 1.0 and decrease with further increase in the relative broken width up to 2.0. For continuous inclined ribs lies close d to friction factor ratio for broken width 2.0, due to very weak flow through this large gap ( $b/e = 2$ ). The maximum value of the Nusselt number was obtained at broken width of 1.0 with a relative broken position 0.25.

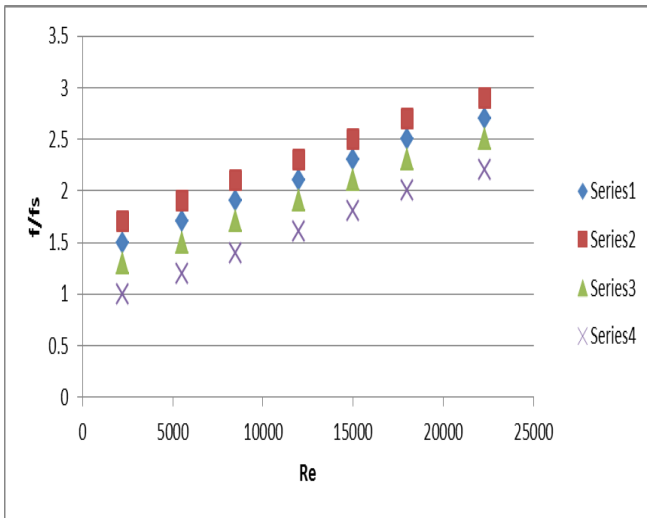


Fig.12. Effect of broken width on friction factor ratio with Reynolds number.

**Correlation for Nusselt number and Friction factor:**

By experimental data it has been observed that Nusselt number and friction factor is function of system and other parameters are Reynolds number (Re), relative roughness pitch (p/e), relative roughness width(W/w) and relative roughness height(e/D).

**Correlation for Nusselt number**

The Nusselt number and Reynolds number have power relationship is shown in fig. From analysis it is found that average slope of all power lines is 1.31. This power line equation represented as

$$Nu = A_0 (Re)^{1.31} \tag{10}$$

The coefficient of A<sub>0</sub> be the function of other influencing parameters. Now parameter e/D taking into consideration and the value of  $\frac{Nu}{(Re)^{1.31}} = A_0$  with respect to e/D graph will be plotted.

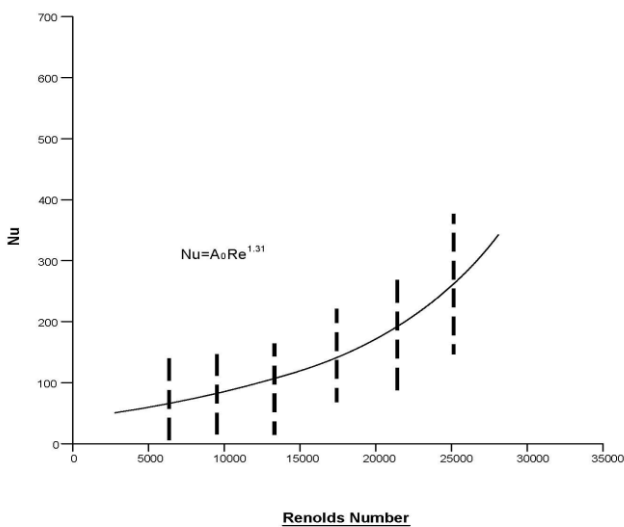


Fig.13. Plot of Nusselt number (Nu) vs Reynolds number(Re)for range of relative roughness pitch.

$$\frac{Nu}{(Re)^{1.31} (\frac{e}{D})^{0.43}} = B_0 \tag{11}$$

For second order curative is obtained

$$\log\left(\frac{Nu}{(Re)^{1.31} (\frac{e}{D})^{0.43}}\right) = \log C_0 + C_1 (\log(p/e)) + C_2 (\log(p/e))^2$$

This equation rearrange in

$$\frac{Nu}{(Re)^{1.31} (\frac{e}{D})^{0.43}} = C_0 \left(\frac{p}{e}\right)^{2.86} [\exp(-0.71(\ln(\frac{p}{e}))^2)] \tag{12}$$

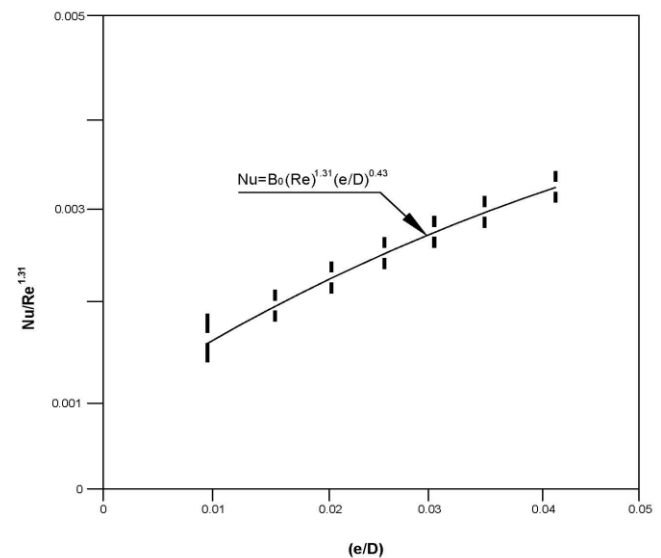


Fig.14. Plot of Nu/Re<sup>1.31</sup> with relative roughness height (e/D). Where, C<sub>0</sub> is the function of ϕ/10. Here the normalizing angle of 10° represents the point where maximum in Nusselt number.

$$\frac{Nu}{(Re)^{1.31} (\frac{e}{D})^{0.43} (\frac{p}{e})^{2.86} [\exp(-0.71(\frac{p}{e})^2)]} = C_0$$

The equation can be rearrange by

$$\frac{Nu}{(Re)^{1.31} (\frac{e}{D})^{0.43} (\frac{p}{e})^{2.86} [\exp(-0.71(\ln(\frac{p}{e}))^2)]} =$$

$$D_0 \left(\frac{\phi}{10}\right)^{-0.018} [\exp(-1.50(\ln(\frac{\phi}{10}))^2)] \tag{13}$$

The value of coefficient is

$$A_0 = 7.46 \times 10^{-4}, \quad B_0 = 3.9 \times 10^{-3}, \quad C_0 = 1.9 \times 10^{-4}, \quad D_0 = 1.89 \times 10^{-4}$$

These result in following relationship for the Nusselt number are

$$Nu = 1.89 \times$$

$$10^{-4} (Re)^{1.31} (\frac{e}{D})^{0.43} (\frac{p}{e})^{2.86} [\exp(-0.71(\ln(\frac{p}{e}))^2)] \left(\frac{\phi}{10}\right)^{-0.018} [\exp(-1.50(\ln(\frac{\phi}{10}))^2)] \tag{14}$$

Fig.10. Plot of predicted value vs. Experimental value of Nusselt number.

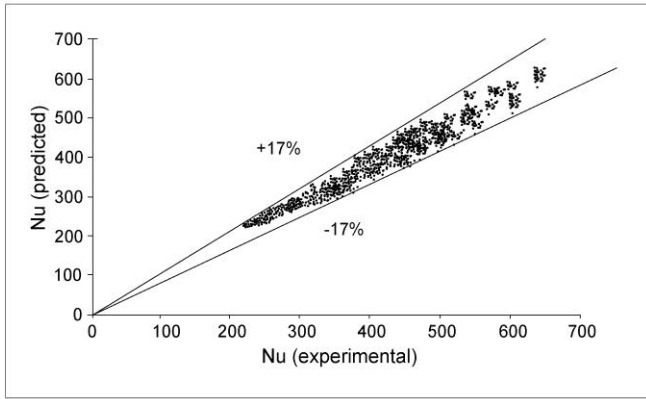


**Fig.15.** Plot of predicted value vs. Experimental value of Nusselt number.

**Correlation for Friction factor**

Similarly, developed a correlation for the friction factor.

$$A_{11}=0.15, B_{11}=4.11, C_{11}=12.57$$

And the final correlation for friction factor can be written as

$$f = 12.44 (Re)^{-0.17} \left(\frac{e}{D}\right)^{0.96} \left(\frac{p}{e}\right)^{-0.49} \left(\frac{\phi}{10}\right)^{0.47} \quad (15)$$

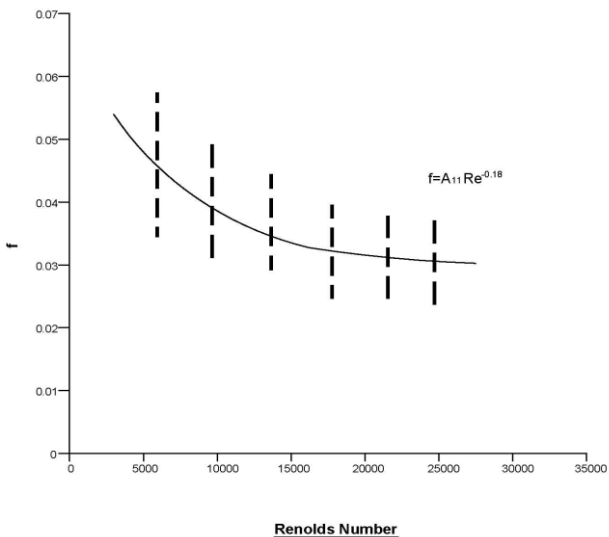


**Fig.16.** Plot of friction factor(f) vs Reynolds number(Re).

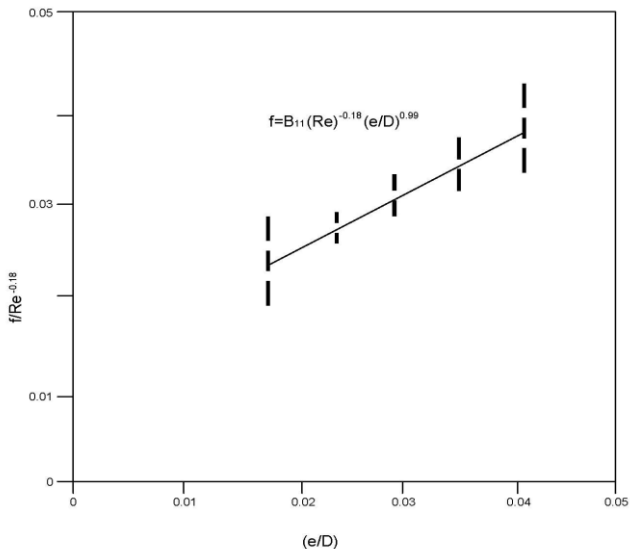


**Fig.17.** Plot of  $f/Re^{-0.18}$  vs relative roughness height (e/D).

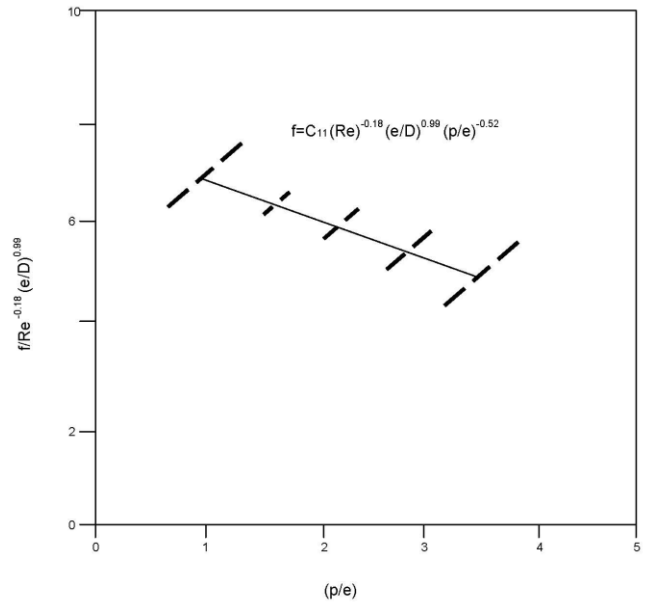


**Fig.18.** Plot of  $f/Re^{-0.18} (e/D)^{0.99}$  vs relative roughness pitch(p/e).

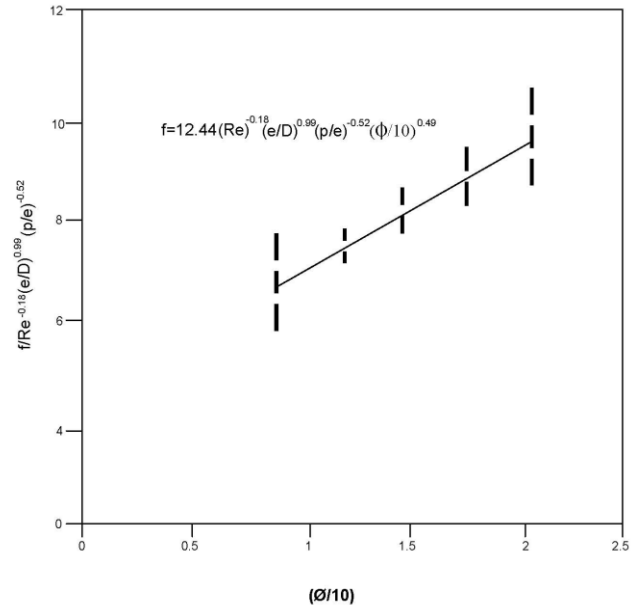


**Fig.19.** Plot of  $f/Re^{-0.18} (e/D)^{0.99} \left(\frac{p}{e}\right)^{-0.52}$  vs  $(\phi/10)$ .

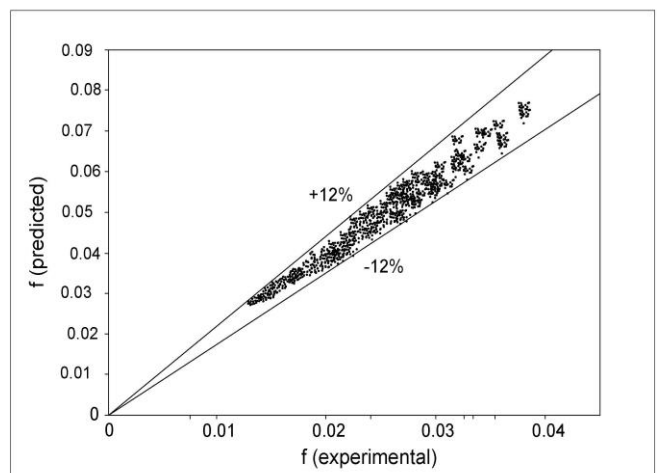


**Fig.20.** Plot of predicted value vs. Experimental value of friction factor.

#### IV. CONCLUSIONS

By experimental observation on 60° inclined rectangular duct rib roughened with and without broken can conclude that:

1. The increase in Nusselt number and friction factor is in the range of 1.47-2.57 times and 2.25-2.9 times of the smooth duct, respectively for the range of Reynolds number 3,000 to 22,300.
2. The maximum enhancement of Nusselt number (Nu) takes place at Reynolds number (Re) of 22,300, relative roughness width at 5, relative roughness height at 0.045, relative roughness pitch 8.
3. The maximum friction factor obtained at Reynolds number of 22300, relative roughness width of 7, relative roughness height of 0.045 and relative roughness pitch of 8.
4. Correlation for Nusselt number and friction factor have been function of rib spacing, rib height, rib angle and Reynolds number. From these correlation found that predicted values within the error limit of  $\pm 17\%$  and  $\pm 12\%$ .

#### REFERENCES

- [1] Bhatti MS, Shah RK. Turbulent and transition flow convective Heat transfer handbook of single-phase convective heat Transfer. New York: Wiley; 1987
- [2] A. Lanjewar, J.L. Bhagoria, R.M. Sarviya, Experimental study of augmented heat transfer and friction in solar air heater with different orientation of W-Rib roughness, Exp. thermal fluid Sci. 35 (2011) 986-995.
- [3] Varun, R.P. Saini, S.K. Singal, A review on roughness geometry used in solar air heater, Sol. Energy 81 (2007).
- [4] V.S. Hans, R.P. Saini, J.S. Saini, performance of artificially roughened solar air heaters- a review, Renew. Sustain. Energy Rev. 13 (2009) 1854-1869.
- [5] A. Kuumar, R.P. Saini, J.S. Saini, Heat and fluid flow Characteristics of roughened solar air heater ducts- a review, Renew. Energy 47 (2012) 77-94.
- [6] M.K. Mittal, Varun, R.P. Saini, S.K. Singal, Effective Efficiency of solar air heaters having different roughness geometry on absorber plate, Energy 32 (2007) 739-745.
- [7] S. Yadav, M. Kaushal, Varun, Siddhartha, Nusselt number and friction factor correlations for solar air heater duct having Protrusions as roughness elements on absorber plate, Exp. Therm. Fluid Sci. 44 (2013) 34-41.
- [8] M. Sethi, Varun, N.S. Thakur, Correlations for solar air heater duct with dimpled shape roughness elements on absorber plate, Sol. Energy 86 (2012) 2852-2861.
- [9] A. Kumar, R.P. Saini, J.S. Saini, Development of correlations for Nusslet number and friction factor for solar air heater with Roughened duct having multi v-shaped with gap rib as artificial Roughness, Renew. Energy 58 (2013) 151-163.
- [10] R. Karwa, G. Chitoshiya, performance study of solar air heater having v-down discrete ribs on absorber plate, Energy 55 (2013) 939-955.
- [11] Varun, R.P. Saini, S.K. Singal, Investigation of thermal performance of solar air heater having roughness elements as a combination of inclined and transverse ribs on the absorber plate, Renew. Energy 33(6) (2008) 1398-1405.
- [12] V.S. Hans, R.P. Saini, J.S. Saini, Heat transfer and friction factor correlations for a solar air heater duct roughened artificially with multiple V-ribs, Sol. Energy 84 (2010)898-911.
- [13] ASHARE Standard 93-97, "Method of Testing to Determine The Thermal Performance of Solar Collector", 1977.
- [14] S.J. Kline, F.A. McClintock, Describing uncertainties in single Sample Experiments, Mech. Eng. 75 (1953) 3-8.
- [15] W.M. Rosen, J.P. Hartnett, Handbook of Heat transfer, McGraw Hill, New York, 1973, pp. 7-122.
- [16] S. Kakac, R.K. Shah, W. Aung, Handbook of single Phase convective heat transfer, John Wiley, New York, 2003.
- [17] R.P. Saini, J.S. Saini, Heat transfer and friction factor correlations for artificially roughened ducts with expended metal meshes roughness element, Int. J. Heat Mass Transfer.40 (1997) 973-986.
- [18] Karwa R. Experimental studies of augmented heat transfer and Friction is asymmetrically heated rectangular ducts with rib on the heated wall in transverse, inclined, V-continuous and V-discrete pattern. Int J Heat Mass Transfer 2003; 30(2):241-50.
- [19] Lau SC, McMillin RD, Han JC. Turbulent heat transfer and friction in a square channel with discrete rib tabulators. Trans ASME, J Turbo machinery 1991; 113:360-6.
- [20] Anil P. Singh, Varun, Sidhartha. Heat transfer and friction factor correlation for multiple arc shape roughness elements on the absorber plate used in solar heater. Experimental Thermal and Fluid Science 54(2014) 117-126.
- [21] J.L. Bhagoria, J.S.Saini, S.C. Solanki. Heat transfer coefficient and friction factor correlation for rectangular solar air heater duct having transverse wedge shaped rib roughness on the absorber plate. Int. J. Renewable Energy 25 (2002) 341-369.